第 36 卷第 1 期
2017 年 2 月

红外与毫米波学报
J. Infrared Millim. Waves

Vol. 36, No. 1
February, 2017

文章编号: 1001 - 9014(2017)01 - 0010 - 06
DOI: 10.11972/j.issn.1001 - 9014.2017.01.003

# Uncertainty in normal reflection terahertz spectroscopy measurement

YANG Fei[1*], LIU Li-Ping[1], SONG Mao-Jiang[1], HAN Feng[1], SHEN Li[1], HU Peng-Fei[1], ZHANG Fang[2*]

(1. Guizhou Institute of Metrology, Guiyang 550003, China;
2. Dept. of Biochemical engineering, Guiyang Vocational and Technical College, Guiyang 550081, China)

**Abstract**: Terahertz time-domain spectroscopy (THz-TDS) is a significant technique for characterizing materials as it allows fast and broadband measurement of optical constants in the THz regime. The measurement precision of the constants is highly influenced by the complicated measurement procedure and data processing. With particular emphasis on normal reflection measurement, the sources of error including amplitude errors and positioning error and sample misalignment in determining the dielectric properties of materials were analyzed. The uncertainty that characterizes the influence on the optical constants for each source was formulated independently. Several simulations were carried out to illustrate the relations between the error sources and the uncertainty of the optical constants.

**Key words**: THz, time-domain spectroscopy (TDS), normal reflection, measurement uncertainty, optical constant
**PACS**: 06.20.DK, 07.57.Pt

# 正入射反射式太赫兹光谱测量的不确定度分析

杨 霏[1*], 刘丽萍[1], 宋茂江[1], 韩 锋[1], 沈 力[1], 胡鹏飞[1], 张 放[2*]

(1. 贵州省计量测试院, 贵州 贵阳 550003;
2. 贵阳职业技术学院生化工程系, 贵州 贵阳 550081)

**摘要**:太赫兹时域光谱技术能够快速、宽频带测量物质在太赫兹频段的光学或介电常数,是物质识别的重要技术.光学常数的测量准确度完全受到复杂的测量过程和数据处理所影响.针对正入射反射式 THz 光谱测量,分析了在测量材料介电特性过程中的误差来源,它们包括太赫兹幅值误差、位置误差以及样品倾斜误差.建立了单独表征每个误差来源对于光学常数影响的不确定度分量的公式.利用 MATLAB 仿真了每个误差来源对于光学参数不确定度的影响.

**关 键 词**:太赫兹;时域光谱;正反射;测量不确定度;光学常数

**中图分类号**:O433.1 **文献标识码**:A

## Introduction

In the past decades, the terahertz time-domain spectroscopy (THz-TDS) has become a powerful tool to measure materials' optical constants in the THz domain. There are two configurations of measurement mode in a THz-TDS system. One is the transmission mode which has been applied to measure various materials effectively, including solids[1], liquids[2] and gases[3]. However, it cannot be used for some substances with high absorption, such as polar liquids and metallic materials, and optically thick samples. These substances can be measured by implementing the reflection measurement. The normal incidence configuration[4-5] with a normal incidence of the THz field onto the sample surface is a widely used reflection measurement. Keiding[6-7] and coworkers proposed a reflection geometry where the full set of spectroscopic data is obtained within the same temporal scan. A reflection spectroscopic technique called attenuated total reflection (ATR)[8-11], which provides information on the interaction between the sample and the evanescent wave traveling along a prism surface, is also widely used.

According to the measurement theory, many sources of error in the THz-TDS measurement process affect the accuracy of extracted optical constants. Many researchers have devoted to assess the influence of errors on optical

**Received date**: 2016-05-11, **revised date**: 2016-07-05 **收稿日期**:2016-05-11, **修回日期**:2016-07-05
**Foundation items**: Supported by National Natural Science of China (21503045, 61540038), and Guizhou Science and Technology Department (J20142107, SY20143065)
**Biography**: Yang Fei (1986-), male, Chongqing, China, Ph. D. Research area is THz spectroscopy, and metrology.
* **Corresponding author**: E-mail: yfl8610@mail.ustc.edu.cn, cafeznse@126.com

constants in several THz-TDS system. For instance, in transmission THz-TDS system the systematic research of errors and their uncertainties contributed to the measured optical parameters was addressed by Duvillaret *et al*[12]. The further researches were given in much greater detail in two papers by Withayachumnankul *et al.* [13-14]. A. Soltani *et al.* [15] calculated the effect of delay errors numerically in THz-ATR system and found that delay fluctuation can be minimized by good thermal stability of the terahertz system. Reference [16] proposed an alternative configuration for ATR THz-TDS that significantly reduces the impact of prism misalignment between the reference and sample measurements. The resembling research for normal reflection terahertz spectroscopy measurement has not been explored to our knowledge. This motivates us to analyze the errors and derive their relations to the uncertainty of measured optical constants in normal reflection terahertz spectroscopy measurement in this work. The influence of amplitude errors and positioning error and sample misalignment are analyzed. It is noted that the influence of divergence of focused THz beam is not taken into account since its uncertainty component is about $10^{-4}$ of dielectric constants[16], which is negligible in determining the dielectric properties of materials.

The remainder of the paper is organized as follows. Section 2 describes the normal reflection terahertz spectroscopy, and derives the measurement functions of optical parameters. In Sect. 3 the sources of error in the THz-TDS measurement and parameter extraction process are identified and their uncertainties are formulated. A numerical study of the developed uncertainty model is given in Sect. 4. A brief conclusion is made in Sect. 5.

## 1 Optical constants measured by normal reflection THz-TDS

As shown in Fig. 1, a femtosecond laser pulse train is split into a pump and probe beam by a beam splitter. The pump beam focuses on the emitter antenna to generate the THz pulse, and the probe beam is delayed by a delay line controlled by a stepping motor to sample the electrical field of the THz signal. The waveform reflected from an ideal mirror is reference signal. The waveform reflected from the sample that is placed at the same place is sample signal.

By Fourier-transforming the two THz waveforms, the spectral components at angular frequency of the electric field are denoted as $E_{ref}(\omega)$ and $E_{sam}(\omega)$, respectively. Then the complex refractive index of the sample can be obtained by the relation

$$\tilde{R}(\omega) = \frac{E_{sam}(\omega)}{E_{ref}(\omega)} = Re^{i\phi_R} = \frac{\tilde{n}-1}{\tilde{n}+1} \quad , \quad (1)$$

where $R$ is the reflectivity and $\phi_R$ is the phase shift between the reference signal and sample signal. $\tilde{n} = n - j\kappa$ is the complex refractive index of the sample with $n$ and $\kappa$ being the refractive index and the extinction coefficient, respectively.

By inverting Eq. (1), one can get analytical expressions of $n$ and $\kappa$ as

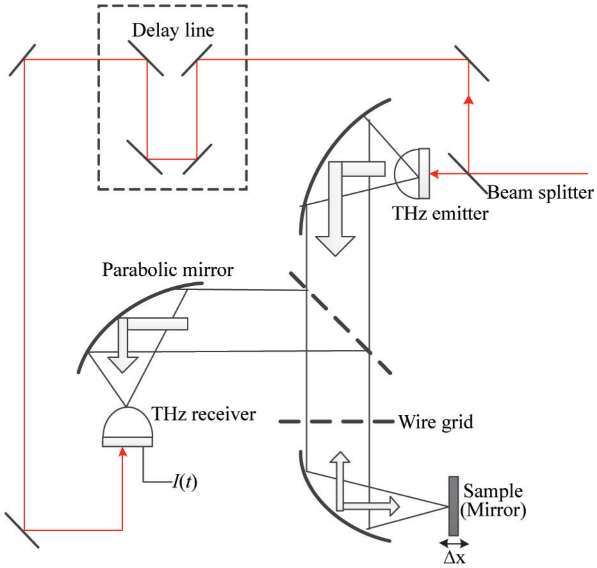


Fig. 1 Schematic of the normal reflection-type THz-TDS
图 1 正入射反射式太赫兹时域光谱示意图

$$n(\omega) = \frac{1-R(\omega)^2}{1+R(\omega)^2-2R(\omega)\cos\phi_R(\omega)} \quad , \quad (2a)$$

$$\kappa(\omega) = \frac{2R(\omega)\sin\phi_R(\omega)}{1+R(\omega)^2-2R(\omega)\cos\phi_R(\omega)} \quad . \quad (2b)$$

The optical constants $n$ and $\kappa$ can be extracted via Eqs. (2a) and (2b) in a normal reflection THz-TDS measurement process and from now on the two equations will be referred to as the measurement functions.

## 2 Uncertainty in THz-TDS reflection measurement

The delay positioning error combined with electronic and optical noise, will give rise to error of amplitude in the time trace. The amplitude error propagates through the Fourier transform and de-convolution stages, to the output uncertainty of optical constants. As discussed in Ref. [17], an even small misalignment of the reference mirror as compared with the position of the sample, will causes a severe error in the deduced complex refractive index in the THz region. Thus, the uncertainties by this error made on the optical properties of the tested sample will be analyzed. In the measurement procedure, the error from the manual placement of sample may give rise to nonzero incident angle. This error also gives rise to the uncertainty of optical constants. Subsections 2.1-2.3 provide an analysis for each source of error in detail.

### 2.1 Errors in T-ray Amplitude

The amplitude-related variance in the refractive index can be calculated as

$$s_{n,E}^2(\omega) = \left(\frac{\partial n}{\partial R}\right)^2 s_{R,E}^2 + \left(\frac{\partial n}{\partial \phi_R}\right)^2 s_{\phi_R,E}^2 \quad , \quad (3)$$

where

$$\frac{\partial n}{\partial R} = \frac{2\cos\phi_R(1+R^2)-4R}{(1+R^2-2R\cos\phi_R)^2} \quad , \quad (4a)$$

$$\frac{\partial n}{\partial \phi_R} = \frac{-2R\sin\phi_R(1-R^2)}{(1+R^2-2R\cos\phi_R)^2} \quad . \quad (4b)$$

Given that the amplitude variances of the time-domain reference and sample signals is denoted by $s^2_{E_{ref}}$ and $s^2_{E_{sam}}$ respectively, according to Ref. [12], the variances of the magnitude and phase of complex reflectivity coefficient are

$$s^2_{R,E}(\omega) = \frac{1}{|E_{ref}(\omega)E_{sam}(\omega)|^2}A_{sam}(\omega) + \frac{|E_{sam}(\omega)|^2}{|E_{ref}(\omega)|^6}A_{ref}(\omega) \quad , \quad (5a)$$

$$s^2_{\phi_R,E}(\omega) = \frac{1}{|E_{sam}(\omega)|^4}B_{sam}(\omega) + \frac{1}{|E_{ref}(\omega)|^4}B_{ref}(\omega) \quad , \quad (5b)$$

where

$$A_{sam}(\omega) = \sum_k \Im^2[E_{sam}(\omega)\exp(j\omega k\tau)]s^2_{E_{sam}}(k) \quad ,(6a)$$

$$A_{ref}(\omega) = \sum_k \Im^2[E_{ref}(\omega)\exp(j\omega k\tau)]s^2_{E_{ref}}(k) \quad ,(6b)$$

$$B_{sam}(\omega) = \sum_k \Re^2[E_{sam}(\omega)\exp(j\omega k\tau)]s^2_{E_{sam}}(k) \quad ,(6c)$$

$$B_{ref}(\omega) = \sum_k \Re^2[E_{ref}(\omega)\exp(j\omega k\tau)]s^2_{E_{ref}}(k) \quad ,(6d)$$

where $\Im^2$ and $\Re^2$ represent the square of the imaginary and real parts, respectively. The sampling interval is denoted by $\tau$, and $k\tau$ represents the sampling time with $k$ being the temporal index.

Substituting Eqs. (4) and (5) into Eq. (3), the amplitude-related variances in the refractive index read as

$$s^2_{n,E}(\omega) = \frac{[2R\cos\phi_R(1+R^2)-4R^2]^2}{(1+R^2-2R\cos\phi_R)^4}\left\{\frac{A_{sam}(\omega)}{|E_{sam}(\omega)|^4}+\frac{A_{ref}(\omega)}{|E_{ref}(\omega)|^4}\right\} + \frac{4(1-R^2)^2R^2\sin\phi_R}{(1+R^2-2R\cos\phi_R)^4}\left\{\frac{B_{sam}(\omega)}{|E_{sam}(\omega)|^4}+\frac{B_{ref}(\omega)}{|E_{ref}(\omega)|^4}\right\} \quad . \quad (7)$$

Likewise, the amplitude-related variances in the extinction index read as

$$s^2_{\kappa,E}(\omega) = \frac{4(1-R^2)^2R^2\sin\phi_R}{(1+R^2-2R\cos\phi_R)^4}\left\{\frac{A_{sam}(\omega)}{|E_{sam}(\omega)|^4}+\frac{A_{ref}(\omega)}{|E_{ref}(\omega)|^4}\right\} + \frac{[4R-2R\cos\phi_R(1+R^2)]^2}{(1+R^2-2R\cos\phi_R)^4}\left\{\frac{B_{sam}(\omega)}{|E_{sam}(\omega)|^4}+\frac{B_{ref}(\omega)}{|E_{ref}(\omega)|^4}\right\} \quad . \quad (8)$$

## 2.2 Errors in Sample Alignment

When the angle of incidence of T-rays on a sample slab is not normal to the surfaces, according to Fresnel equations, the exact complex reflective index of a sample is given by

$$\tilde{R}_{\text{exact}}(\theta) = \frac{\tilde{n}\cos\theta_1 - \cos\theta_2}{\tilde{n}\cos\theta_1 + \cos\theta_2} = R_{\text{exact}}\exp(i\phi_{R,\text{exact}}) \quad ,(9)$$

where $\theta_1$ and $\theta_2$ are the incidence angle and refraction angle, respectively, of THz pulses. According to Snell's law, $n_0\sin\theta_1 = n\sin\theta_2$ holds.

Supposing that the incident angle $\theta_1$ deviates in a small interval $[-f_\theta, f_\theta]$ and has zero arithmetic mean, the magnitude difference and phase difference between the calculated and exact complex reflection coefflcient in the worst-case scenario, are

$$f_{R,\theta}(\omega) = abs(\tilde{R}_{\text{exact}} - \tilde{R}) = \left|\frac{\tilde{n}\cos f_\theta - \cos\left(\arcsin\left(\frac{\sin f_\theta}{n}\right)\right)}{\tilde{n}\cos f_\theta + \cos\left(\arcsin\left(\frac{\sin f_\theta}{n}\right)\right)} - \frac{\tilde{n}-1}{\tilde{n}+1}\right| \quad ,(10)$$

$$f_{\phi_R,\theta}(\omega) = \arg(\tilde{R}_{\text{exact}} - \tilde{R}) = \left|\frac{\tilde{n}\cos f_\theta - \cos\left(\arcsin\left(\frac{\sin f_\theta}{n}\right)\right)}{\tilde{n}\cos f_\theta + \cos\left(\arcsin\left(\frac{\sin f_\theta}{n}\right)\right)} - \frac{\tilde{n}-1}{\tilde{n}+1}\right| \quad .(11)$$

Derived from the measurement functions in Eq. (2), the effect of sample alignment error on the refractive index deviation is

$$f_{n,\theta}(\omega) = \left|\frac{2\cos\phi_R(1+R^2)-4R}{(1+R^2-2R\cos\phi_R)^2}\right| f_{R,\theta} + \left|\frac{2R\sin\phi_R(1+R^2)}{(1+R^2-2R\cos\phi_R)^2}\right| |f_{\phi_R,\theta}| \quad .(12)$$

Likewise, the effect of sample alignment error on the deviation of the extinction coefficient is

$$f_{\kappa,\theta}(\omega) = \left|\frac{2\sin\phi_R(1-R^2)}{(1+R^2-2R\cos\phi_R)^2}\right| f_{R,\theta} + \left|\frac{4R^2-2R\cos\phi_R(1+R^2)}{(1+R^2-2R\cos\phi_R)^2}\right| |f_{\phi_R,\theta}| \quad .(13)$$

## 2.3 Error in the samples' position

The reflection measurement requires the reference measurement using the metal mirror at strictly the same position as that of the sample. This is rather difficult to achieve in real measurements, and the error $\Delta_x$ (see Fig. 1) induced by an even small misalignment induces a phase error:

$$\Delta\phi_R = \frac{2\Delta_x\omega}{c} \quad . \quad (14)$$

Then the deviation in the refractive index and extinction coefficient, respectively, arising from the small misalignment $\Delta_x$, are

$$f_{n,\Delta_x} = \frac{-2R\sin\phi_R(1-R^2)}{(1+R^2-2R\cos\phi_R)^2}\cdot\frac{2\omega}{c}\Delta_x = n(\omega)\alpha(\omega)\Delta_x \quad ,(15a)$$

$$f_{\kappa,\Delta_x}(\omega) = abs\left[\frac{\alpha}{2} - \frac{2\omega^2(n^2-1)}{c^2\alpha}\right]\kappa\Delta_x \quad ,(15b)$$

where $\alpha(\omega) = 2\omega\kappa(\omega)/c$ is the absorption coefficient of the sample.

Regarding Eq. (15), the relative errors made on real and imaginary parts of the complex refractive index are highly related to the absorption coefficient of the sample. The relative error of refractive index $f_{n,\Delta_x}/n$ is larger for more absorbing material. Whereas for relative error of extinction coefficient $f_{\kappa,\Delta_x}/\kappa$ there exists an inflexion value $2\omega\sqrt{n^2-1}/c$ of absorption coefficient, below which

$f_{\kappa,\Delta_x}/\kappa$ is getting smaller when $\alpha$ increases. Above this value, which ranges from tens to hundreds of $cm^{-1}$ in the THz range, $f_{\kappa,\Delta_x}/\kappa$ gets bigger with increasing $\alpha$. Therefore, for a highly absorbing material, the uncertainties due to misalignment made on the optical properties of the tested sample are quite big and deserve to be corrected either by numerical[18] or experimental[19] solutions.

## 3 Impact of individual source of uncertainty

In order to analyze the impact of each source of uncertainty on the overall optical constants' uncertainty, several simulations were carried out. According to the PCA analytical model given by Duvillaret *et al*[20], the T-ray reference and sample signals were simulated with the parameters in Ref. [18]: $\delta\tau_{em} = \delta\tau_{rec} = 30$ fs, $\tau_{em} = \tau_{rec} = 300$ fs, and $\tau_{las} = 120$ fs. The reference pulse has the FWHM of approximately 0.5ps, giving the frequency span from 0.1 THz to 4.0 THz. The sample signal was calculated for the case that the experimental parameters are as follows: $n\text{-}j\kappa = 1.5\text{-}0.1j$. Figure 2 shows the T-ray reference and sample signals simulated according to the PCA analytical.

### 3.1 Error in T-ray amplitude

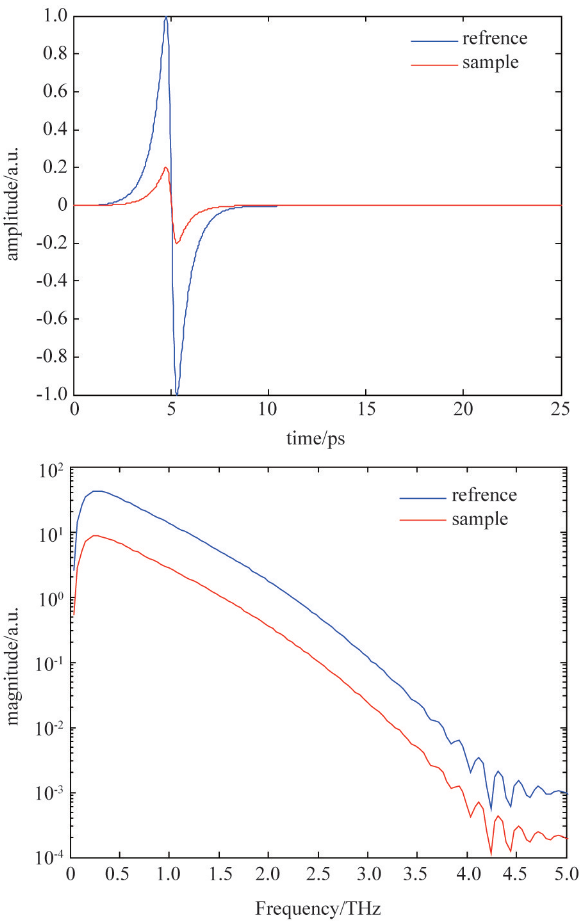


Fig. 2 Simulated T-ray signals and spectra for reference and sample

图 2 仿真的参考信号及样品信号以及它们的频谱

According to Ref. [11], the variances of T-ray's amplitude affected by the noise can be recorded as $AE^2(k\tau) + BE(k\tau) + C$, with A, B, and C being the noise parameters. By fitting the experimental values of the optical constants' variance, they showed that the order of magnitude for A, B, C are about of $10^{-3}$, $10^{-5}$, and $10^{-7}$, respectively. Therefore, the parameters A were chosen from 0.001 to 0.01 with 0.001 increment. The parameters B were chosen from 0.000 01 to 0.000 1 with 0.000 01 increment. And the parameters C were chosen from 0.000 000 1 to 0.000 001 with 0.000 000 1 increment. The corresponding standard deviations of $n$ and $\kappa$ were calculated with Eqs. (7-8) and illustrated in Fig. 3.

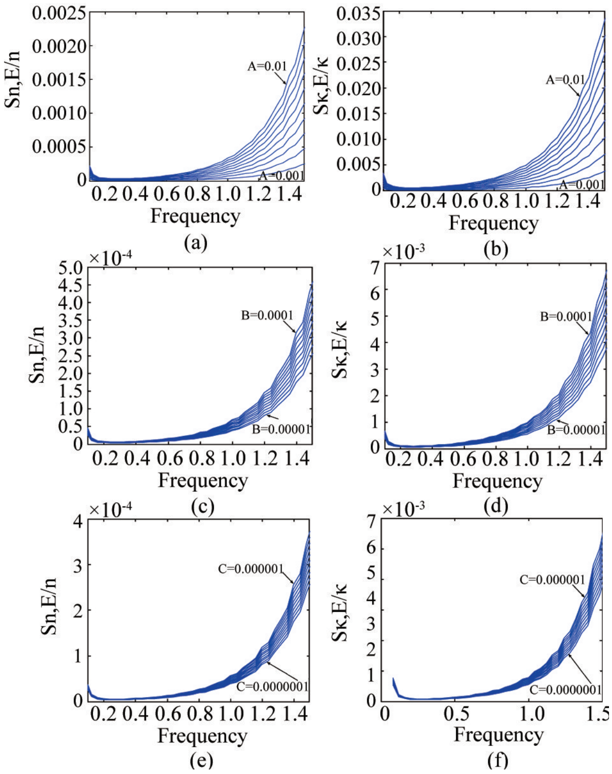


Fig. 3 Standard deviation of optical constants affected by noise characterized by different noise parameters *A*, *B* and *C*. (a) Standard deviation of *n* for different A (b) Standard deviation of *κ* for different A (c) Standard deviation of *n* for different B (d) Standard deviation of *κ* for different B (e) Standard deviation of n for different C (f) Standard deviation of κ for different C

图 3 受不同参数条件的噪声影响下的光学常数的标准差 (a)不同参数 A 对应的 n 的标准差;(b)不同参数 A 对应的 *κ* 的标准差;(c)不同参数 B 对应的 *n* 的标准差;(d)不同参数 B 对应的 *κ* 的标准差;(e)不同参数 C 对应的 n 的标准差;(f)不同参数 C 对应的 *κ* 的标准

It can be seen that the variation of $n$ and $\kappa$ are very small below 1THz, and ascend rapidly at higher frequencies, showing that the uncertainty of refractive index and extinction coefficient are affected by the noise more easily at high frequencies, probably since that higher frequencies are more strongly affected by errors in mirror position and orientation in a THz-TDS. It is noted that, in an actual THz-TDS measurement, the variances of T-ray's amplitude can be obtained by measuring the sample and reference several times.

### 3.2 Error in sample alignment

Figure 4 shows the impact of sample's titling angle on the complex refractive index. The titling angle was chosen from 0.01 to 0.1 with 0.01 increment. The deviations in $n$ and $\kappa$ become larger as the increase of titling angle. The extinction coefficient are more sensitive to the titling angle than refractive index because that $\kappa$ is very related to the phase shift between the reference signal and sample signal, which is strongly dependent on the incident angle of THz beams onto the sample.

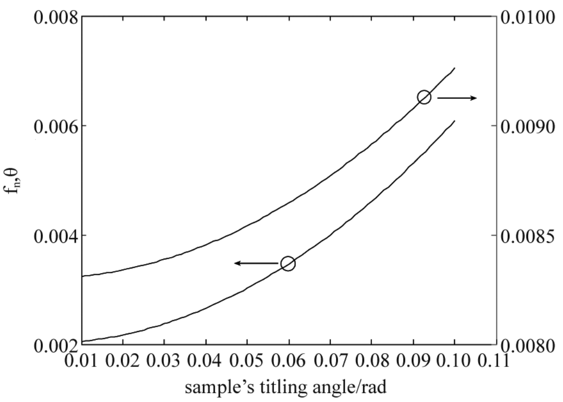


Fig. 4 The deviation in $n$ and $\kappa$ with respect to sample's titling angle
图 4 对应不同样品倾斜角的 $n$ 和 $\kappa$ 的偏差

### 3.3 Impact from positioning error

As is shown in Fig. 5, the positioning error considered here is in the order of a micron. The deviations in optical constants become larger as the positioning error increases, and are small compared with the optical constants at low frequencies. However, at higher frequencies, the deviations rise rapidly to an unacceptable level and become much larger than that caused by the other two errors. It may be conjectured that the positioning error is the major source contributing to the uncertainty of optical constants.

## 4 Conclusion

This paper investigated the sources of error contributing to the measurement uncertainty of optical constants in normal reflection terahertz spectroscopy. The analytical formulas qualifying the relations between error's variance or deviation and that in the optical constants were derived. The relations were illustrated by several simulation results, which showed that the extinction coefficient is more sensitive to the errors than refractive index and the uncertainty of optical constants are larger at higher frequencies. The analysis of uncertainty is expected to shed light on choosing applicable correction method to improve measurement accuracy.

It is noted that a number of optical effects are omitted from the widely used transfer function model, or Eq. (1). These effects, particularly arising from a beam focusing configuration, include frequency-dependent beam shape (beam waist at the focal point, Rayleigh length, beam divergence)[21] and beam defocusing by the sample. Treatment of these effects is appropriate for future work.

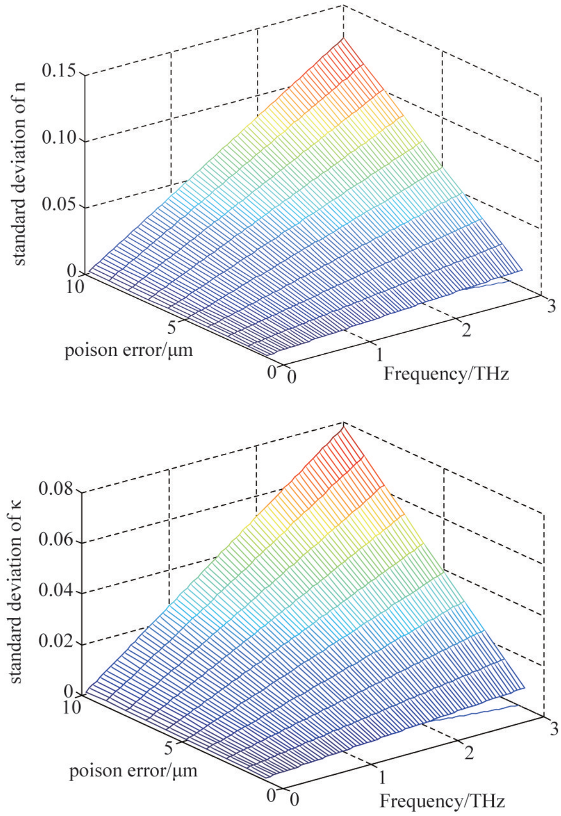


Fig. 5 Deviations in optical constants affected by positioning error which runs from 1 μm to10 μm with 1 μm step size
图 5 不同位置误差(从 1μm 到 10 μm 每隔 1 μm 取值)对应的光学常数的偏差

## References


[1] Tanaka K, Hirori H, Nagai M. THz Nonlinear Spectroscopy of Solids [J]. IEEE Transactions on Terahertz Science & Technology, 2011, **1** (1):301-312.

[2] Federici J F. Review of Moisture and Liquid Detection and Mapping using Terahertz Imaging[J]. Journal of Infrared Millimeter & Terahertz Waves, 2012, **33**(2):97-126.

[3] Hübers H W, Pavlov S G, Richter H, *et al.* High-resolution gas phase spectroscopy with a distributed feedback terahertz quantum cascade laser [J]. Applied Physics Letters, 2006, **89**(6):061115-061115-3.

[4] Hangyo M, Nagashima T, Nashima S. Spectroscopy by pulsed terahertz radiation [J]. Measurement Science & Technology, 2002, **13** (13):1727-1738.

[5] Wang X, Sun W, Zhang Y. A novel normal reflection terahertz spectrometer [J]. Optik, 2010, **121**(12):1148-1153.

[6] Rønne C, Thrane L, Åstrand P O, *et al.* Investigation of the temperature dependence of dielectric relaxation in liquid water by THz reflection spectroscopy and molecular dynamics simulation[J]. Journal of Chemical Physics, 1997, **107**(14):5319-5331.

[7] Jepsen P U, Møller U, Merbold H. Investigation of aqueous alcohol and sugar solutions with reflection terahertz time-domain spectroscopy. [J]. Optics Express, 2007, **15**(22):14717-37.

[10] Hirori H, Yamashita K, Nagai M, *et al.* Attenuated Total Reflection Spectroscopy in Time Domain Using Terahertz Coherent Pulses[J]. Japanese Journal of Applied Physics, 2004, **43**(10A):361-363.


(下转第 19 页)

[18] Liu K, Yu F. Accurate wavelength calibration method using system parameters for grating spectrometers [J]. *Optical Engineering*, 2013, **52**(1): 013603-6.

[19] Emadi A, Wu H, Grabarnik S, *et al*. Fabrication and characterization of IC-Compatible Linear Variable Optical Filters with application in a micro-spectrometer [J]. *Sensors and Actuators A: Physical*, 2010, **162**(2): 400-5.

[20] Keating A, Antoszewski J, Silva K, *et al*. Design and characterization of Fabry-Perot MEMS-based short-wave infrared microspectrometers [J]. J*ournal of electronic materials*, 2008, **37**(12): 1811-20.

[21] Friedrich R, Fischer J, Stock M. Accurate calibration of filter radiometers against a cryogenic radiometer using a trap detector [J]. *Metrologia*, 1995, **32**(6): 509-13.

[22] Lu X, Yuan Z, Hao X, *et al*. Calibration of the Irradiance, Responsivity of a Filter Radiometer for T Measurement at NIM International [J]. *Journal of Thermophysics*, 2011, **32**(1-2): 278-84.

[23] Campos J, Corróns A, Pons A, *et al*. Spectral responsivity uncertainty of silicon photodiodes due to calibration spectral bandwidth [J]. *Measurement Science and Technology*, 2001, **12**(11): 1926-31.

[24] Lamminpää A, Noorma M, Hyyppä T, *et al*. Characterization of germanium photodiodes and trap detector [J]. *Measurement Science and Technology*, 2006, **17**(4): 908-12.

[25] Rogalski A. Progress in focal plane array technologies [J]. *Progress in Quantum Electronics*, 2012, **36**(2): 342-473.

(上接 14 页)

[11] Hirori H, Yamashita K, Nagai M, *et al.* Attenuated Total Reflection Spectroscopy in Time Domain Using Terahertz Coherent Pulses [J]. Japanese Journal of Applied Physics, 2004, **43**(10A): 361-363.

[12] Duvillaret L, Garet F, Coutaz J L. Influence of noise on the characterization of materials by terahertz time-domain spectroscopy [J]. J. Opt. Soc. Amer. B, 2000, **17**(3): 452-461.

[13] Withayachumnankul W, Fischer B M, Lin H, *et al.* Uncertainty in terahertz time-domain spectroscopy measurement [J]. Journal of the Optical Society of America B, 2008, **25**(6): 1059-1072.

[14] Lin H, Mickan S P, Fischer B M, *et al.* Analysis of measurement uncertainty in THz-TDS [J]. Proceedings of SPIE-The International Society for Optical Engineering, 2007, 6593.

[15] Soltani A, Probst T, Busch S F, *et al*. Error from Delay Drift in Terahertz Attenuated Total Reflection Spectroscopy [J]. Journal of Infrared Millimeter & Terahertz Waves, 2014, **35**(5): 468-477.

[16] Yang Fei, Liu Li-Ping, Song Mao-jiang, *et al*. Uncertainty in Terahertz time-domain spectroscopy measurement of liquids [J]. J Infrared Milli Terahz Waves, 2017, **38**(2): 229-247.

[17] Hangyo M, Nagashima T, Nashima S. Spectroscopy by pulsed terahertz radiation [J]. Measurement Science & Technology, 2002, **13**(13): 1727-1738.

[18] Khazan M, Meissner R, Wilke I. Convertible transmission-reflection time-domain terahertz spectrometer [J]. Review of Scientific Instruments, 2001, **72**(8): 3427-3430.

[19] Vartiainen E M, Ino Y, Shimano R, *et al.* Numerical phase correction method for terahertz time-domain reflection spectroscopy [J]. Journal of Applied Physics, 2004, **96**(8): 4171-4175.

[20] Duvillaret L, Garet F, Roux J F, *et al.* Analytical modeling and optimization of terahertz time-domain spectroscopy experiments, using photoswitches as antennas [J]. IEEE Journal of Selected Topics in Quantum Electronics, 2001, **7**(4): 615-623.

[21] Gürtler A, Winnewisser C, Helm H, *et al*. Jepsen, Terahertz pulse propagation in the near field and the far field [J]. J. Opt. Soc. Am. A, 2000, **17**, 74-83.